Journal of Hazardous Materials 470 (2024) 134195

Contents lists available at ScienceDirect

Journal of Hazardous Materials

journal homepage: www.elsevier.com/locate/jhazmat

Bioreduction of chromate in a syngas-based membrane biofilm reactor

Chenkai Niu [a,1], Xinyu Zhao [a,1], Danting Shi [b], Yifeng Ying [a], Mengxiong Wu [a], Chun-Yu Lai [c], Jianhua Guo [a], Shihu Hu [a], Tao Liu [a,b,*]

[a] Australian Centre for Water and Environmental Biotechnology (ACWEB, formerly AWMC), The University of Queensland, St. Lucia, Queensland 4072, Australia
[b] Department of Civil and Environmental Engineering, The Hong Kong Polytechnic University, 999077, Hong Kong Special Administrative Region of China
[c] College of Environmental and Resource Science, Zhejiang University, Hangzhou, Zhejiang 310058, China

HIGHLIGHTS

- Efficient Cr(VI) reduction is achieved in syngas-based MBfR.
- Syngas fermentation produces volatile fatty acids *in situ*.
- Volatile fatty acids drive Cr(VI) reduction primarily and hydrogen plays a minor contribution.

GRAPHICAL ABSTRACT

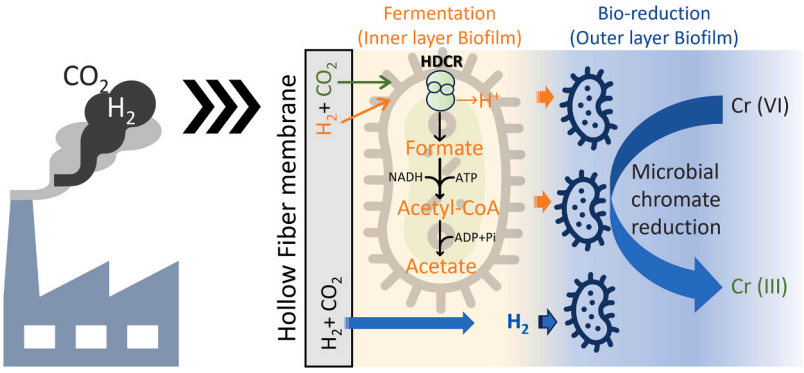

ARTICLE INFO

Keywords:
Syngas
Fermentation
Membrane biofilm reactor (MBfR)
Chromate reduction
Groundwater remediation

ABSTRACT

This study leveraged synthesis gas (syngas), a renewable resource attainable through the gasification of biowaste, to achieve efficient chromate removal from water. To enhance syngas transfer efficiency, a membrane biofilm reactor (MBfR) was employed. Long-term reactor operation showed a stable and high-level chromate removal efficiency > 95%, yielding harmless Cr(III) precipitates, as visualised by scanning electron microscopy and energy dispersive X-ray analysis. Corresponding to the short hydraulic retention time of 0.25 days, a high chromate removal rate of 80 μmol/L/d was attained. In addition to chromate reduction, *in situ* production of volatile fatty acids (VFAs) by gas fermentation was observed. Three sets of *in situ* batch tests and two groups of *ex situ* batch tests jointly unravelled the mechanisms, showing that biological chromate reduction was primarily driven by VFAs produced from *in situ* syngas fermentation, whereas hydrogen originally present in the syngas played a minor role. 16 S rRNA gene amplicon sequencing has confirmed the enrichment of syngas-fermenting bacteria (such as *Sporomusa*), who performed *in situ* gas fermentation leading to the synthesis of VFAs, and organics-utilising bacteria (such as *Aquitalea*), who utilised VFAs to drive chromate reduction. These findings, combined with batch assays, elucidate the pathways orchestrating synergistic interactions between fermentative microbial cohorts and chromate-reducing microorganisms. The findings facilitate the development of cost-

* Corresponding author at: Australian Centre for Water and Environmental Biotechnology (ACWEB, formerly AWMC), The University of Queensland, St. Lucia, Queensland 4072, Australia.
E-mail address: uqtliu8@uq.edu.au (T. Liu).
[1] These authors contributed equally to the work

https://doi.org/10.1016/j.jhazmat.2024.134195
Received 2 January 2024; Received in revised form 7 March 2024; Accepted 31 March 2024
Available online 2 April 2024

effective strategies for groundwater and drinking water remediation and present an alternative application scenario for syngas.

1. Introduction

Chromium (Cr) pollution has been commonly detected in surface water and groundwater because of its wide use in various industries, such as petroleum refining, stainless steel and refractory material manufacturing, and chemical synthesis [6,69,7]. Chromate (Cr(VI)) is a toxic form of Cr. Upon penetrating cell membranes, Cr(VI) interacts with proteins, inhibiting the activity of specific enzymes [50]. It also has the potential to react with nucleic acids, disrupting the metabolism of normal cells, leading to cardiovascular shock, liver, and kidney necrosis [47,51]. Additionally, exposure to Cr(VI) can instigate the generation of free radicals and reactive oxygen species (ROS) [66]. ROS, in turn, directly induces DNA damage, gene mutations, and an increase in pro-inflammatory cytokines, thereby precipitating cancer and inflammation. As such, a maximum level of 100 μg/L has been set for Cr in drinking water by the US Environmental Protection Agency.

Biological reduction of chromate to trivalent Cr (Cr(III)) is a promising solution for chromate removal [20,40]. Compared to the physicochemical remediation of chromate, biological methods have the advantages of sustainability and low cost, thus attracting significant interest [18,40]. Various organic (*e.g.*, methanol, acetate, and lactate) [30,56,63] and inorganic (H_2 and elemental sulfur) [14,61] electron donors have been used for microbial chromate reduction. In terms of the microorganisms responsible for chromate reduction, phylogenetically diverse bacteria, including *Pseudomonas* sp., *Desulfovibrio* sp., *Staphylococcus epidermidis*, *Arthrobacter* sp., and *Escherichia coli* have been identified as capable of reducing Cr(VI) to Cr(III) [3,44,45,60,71]. The formed Cr (III) can easily precipitate at a neutral or high pH, facilitating Cr removal and recovery [29,42].

Although the use of organic substances as electron sources generally achieves stable and high Cr(VI) removal efficiency, the cost of organics cannot be ignored [68]. H_2 and CH_4, obtained by water splitting and anaerobic sludge digestion, respectively, have been proposed as cost-effective electron sources for Cr(VI) bioremediation [14,29,42]. In membrane biofilm reactors (MBfRs), H_2 or CH_4 is delivered through bubble-free hollow fibre membranes, enabling high gas utilisation efficiency. In addition to H_2 and CH_4, syngas, which is a gas mixture comprising H_2, CO, and CO_2, can be produced from the gasification of a diverse range of carbonaceous feedstocks and is thus a widely available and renewable electron and carbon source [65,67]. However, whether syngas can be used to remove Cr(VI) from contaminated waters remains unknown.

This study aimed to develop a syngas-based MBfR for Cr(VI) bioremediation. To this end, an MBfR was set up with hollow fibre membranes to supply syngas and enable biofilm attachment. Initially, synthetic influent containing nitrate and ammonium was fed into the reactor to facilitate biofilm development. Afterwards, the reactor was continuously supplied with Cr(VI) at a hydraulic retention time (HRT) of 0.1–0.5 days to evaluate the long-term chromate removal performance. Multiple *in situ* and *ex situ* batch tests were performed to elucidate the mechanisms of chromate removal in the syngas-based MBfR. The key microbial populations involved in syngas-driven chromate reduction were investigated using 16 S rRNA gene amplicon sequencing.

2. Material and methods

2.1. Syngas-based MBfR setup

A laboratory-scale MBfR (Fig. 1) with a total effective volume of 100 mL was designed for continuous chromate removal. In the MBfR setup, three sets of hollow fibre membranes (model MHF-200TL, Mitsubishi, Ltd., Tokyo, Japan) were incorporated for gas delivery, as outlined in Table S1. Following previous studies [55,57,77], syngas comprising 80% H_2 and 20% CO_2 was introduced into the MBfR through the upper end of the fibre bundle. No CO was supplied in this laboratory proof-of-concept study, owing to safety concerns. The opposite end of the bundle was sealed to ensure exclusive gas permeation towards the biofilm from the hollow fibre membrane. The bulk liquid inside the MBfR and overflow bottle was effectively mixed using a peristaltic pump (BT300–2 J, Longer Pump, Hebei, China) at a constant liquid flow rate of 20 mL/min. Monitoring of the pH levels and sampling of both gases and liquids were conducted in an overflow bottle. The entire syngas-based

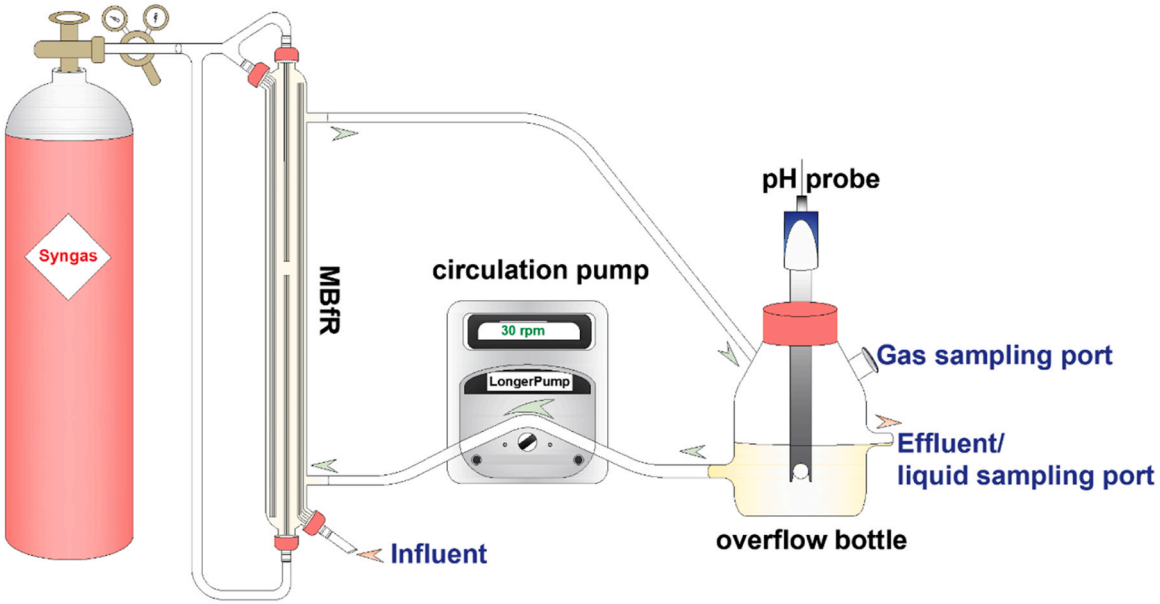

Fig. 1. Schematic of syngas-based MBfR.

MBfR was operated in a temperature-controlled laboratory at 21 ± 1 °C. The potential reactions for gas fermentation and chromate removal are described in Eqs. 1 and 2.

$$4H_2 + 2CO_2 \rightarrow CH_3COOH + 2H_2O \quad (1)$$

$$8CrO_4^{2-} + 40H^+ + 3CH_3COOH \rightarrow 8Cr^{3+} + 6CO_2 + 26H_2O \quad (2)$$

2.2. Inoculum and mineral medium

A mixture of 10 mL of activated sludge and 10 mL of anaerobic digestion sludge obtained from the Luggage Point wastewater treatment plant (Brisbane, Australia) was inoculated into the MBfR. The mineral salts used in the synthetic influent in Stages I and II are listed in Table S2. The difference between these two stages was the addition of either N or Cr(VI) compounds.

2.3. Long-term operation

The long-term operation was divided into two stages, each tailored to specific objectives: Stage I focused on biofilm development, while Stage II targeted chromate removal. In the early part of the first stage (day 1–20), continuous feeding was initially avoided to prevent biomass washout and promote biofilm formation. To sustain microbial activity, regular dosing with 1 mL of 30 g/L sodium nitrate stock solution was performed. On day 21, synthetic wastewater containing 600 mg NO_3^--N/L and 100 mg NH_4^+-N/L was introduced into the MBfR. Nitrate has been used as a substrate for biofilm development in MBfR in a previous study [42]. The HRT was gradually reduced from 2 days to 1 during this stage.

After successful biofilm development, the influent was switched to chromate-containing synthetic wastewater. In Stage II, a feed of 20 μmol/L chromate was initiated from day 68, and the HRT was manually adjusted to 0.5 days without any adaptation. Throughout the long-term operation, the influent and effluent were regularly analysed for chromate, nitrate, nitrite, ammonium, and volatile fatty acid (VFA) concentrations, 1–3 times weekly. Additionally, biofilm samples were collected at the end of Stages I and II for microbial community analyses. Details of the chemical and microbial analyses can be found in Texts S1 and S2 of the Supplemental Information.

2.4. In situ batch tests

The long-term performance of Cr(VI) removal from the syngas-based MBfR was confirmed, followed by two sets of *in situ* batch assays (A and B) to further elucidate the roles of syngas and VFAs in Cr(VI) removal (Table S3). Continuous feeding was terminated before each batch assay. In batch test A, various chromate concentrations (5–30 μmol/L) were applied to the MBfR to measure the Cr(VI) reduction rate in the presence of syngas and VFAs. In the negative control group (batch B), the syngas supply was discontinued, and fresh medium was introduced to remove residual VFAs from the MBfR. Cr(VI) (10 μmol/L) was added to observe whether its removal could persist in the absence of syngas and VFAs. Another control group with acetate but without syngas was performed to validate the role of VFAs in Cr(VI) reduction (batch C). In this test, the initial acetate concentration was about 70 mg/L. The Cr(VI) was dosed into the reactor to reach an initial concentration of about 6 μmol/L. After 7 h, the Cr(VI) was re-dosed again to repeat the experiment. Liquid samples were collected at regular intervals during each batch test to monitor changes in the Cr(VI) and VFA concentrations over time.

2.5. Ex situ batch tests

To understand the specific contributions of H_2 and CO_2 to the Cr (VI) removal process, two sets of *ex situ* experiments were conducted (Table S3). Microorganisms adhering to the membrane were scrupulously removed and homogeneously mixed. Subsequently, the six serum bottles were flushed with nitrogen gas for 10 min to create an anaerobic environment. The obtained biomass was evenly divided into six serum bottles. In batch test D, 50 mL H_2 was injected, whereas in batch test E, a mixture of 50 mL H_2 and 10 mL CO_2 was introduced. Subsequently, the liquid was mixed using magnetic stirrers at 300 rpm for 5 min to ensure equilibrium of H_2 and CO_2 between the gas and liquid phases. Subsequently, a stock solution of Cr(VI) was introduced into the serum bottles, achieving an initial Cr(VI) concentration of approximately 20 μmol/L. Over the 25 h *ex situ* batch tests, liquid and gas samples were regularly collected to determine the Cr(VI) reduction and gas consumption rates. To compare the differences observed in various batch tests, statistical analysis was performed using a one-way analysis of variance within the framework of GraphPad Prism software. Statistical significance was set at $p < 0.05$.

2.6. Observation of the Cr (III) precipitates

The Cr(III) precipitates were examined using scanning electron microscopy (SEM) and energy-dispersive X-ray spectroscopy (EDS) using a JEOL JSM-7100 F instrument (Tokyo, Japan). To enhance the visibility of the Cr precipitates on the biofilm, the sample extracted from the MBfR was thoroughly washed with ethanol to eliminate any adhering slime. Subsequently, the specimen was air-dried at ambient temperature, followed by the application of a platinum coating to facilitate optimal visualisation of electron aggregation.

3. Results and Discussion

3.1. Biofilm development, DNRA, and VFA production in syngas-based MBfR

In Stage I, nitrate was completely removed without nitrite accumulation as the HRT was gradually decreased from 2 days to 1 (Fig. 2a), resulting in a peak total nitrogen removal rate of approximately 600 mg N/L/d (Fig. 2b). In contrast, the influent ammonium was not efficiently consumed, and the ammonium concentration in the effluent was unexpectedly higher than that in the influent. This observation suggests the occurrence of dissimilatory nitrate reduction to ammonium (DNRA) in the syngas-based MBfR. DNRA is typically observed in environments rich in electron donors but limited in nitrate [74], which has also been reported in previous MBfRs fuelled by methane [35,49]. To investigate the factors influencing the DNRA process, the partial pressure of the syngas was reduced from 1.5 to 1.3 atm on day 54. Following this adjustment, the ammonium concentration in the effluent decreased to < 100 mg N/L after day 57. This indicates that syngas provision regulates the balance between DNRA and denitrification. Over time, a biofilm layer gradually formed on the hollow fibre surface during Stage I, whereas no suspended biomass was observed in the bulk liquid.

Furthermore, VFA production was also observed in the syngas-based MBfR. Acetate was the predominant fatty acid detected in the system, accompanied by low levels of propionate and butyrate (Fig. 2c–d). Specifically, the acetate concentration fluctuated between 100 mg/L and 300 mg/L during the initial 50 days, peaking at 1250 mg/L on day 57 likely due to the enrichment or adaptation of fermenting bacteria. Reducing gas supply after day 54 adversely affected fermenting bacteria, leading to the decrease of acetate to 484 mg/L at the end of Stage I. This finding provides preliminary evidence of VFA production in syngas-based MBfRs. The bioconversion of syngas to VFAs, also known as syngas fermentation, is a well-established process [34,75]. However, previous studies have typically employed highly enriched cultures or isolated strains for syngas fermentation [16,17,24,53,72]. Additionally, attaining VFAs accumulation typically requires inhibition of the methanogenic pathway, which is achieved through the addition of specific inhibitors (*e.g.*, 2-bromoethanesulfonate and/or the implementation of harsh conditions (*e.g.*, acidic or alkaline conditions) [36,80]. In the present study, the methane percentage in the off-gas was only 1–3%,

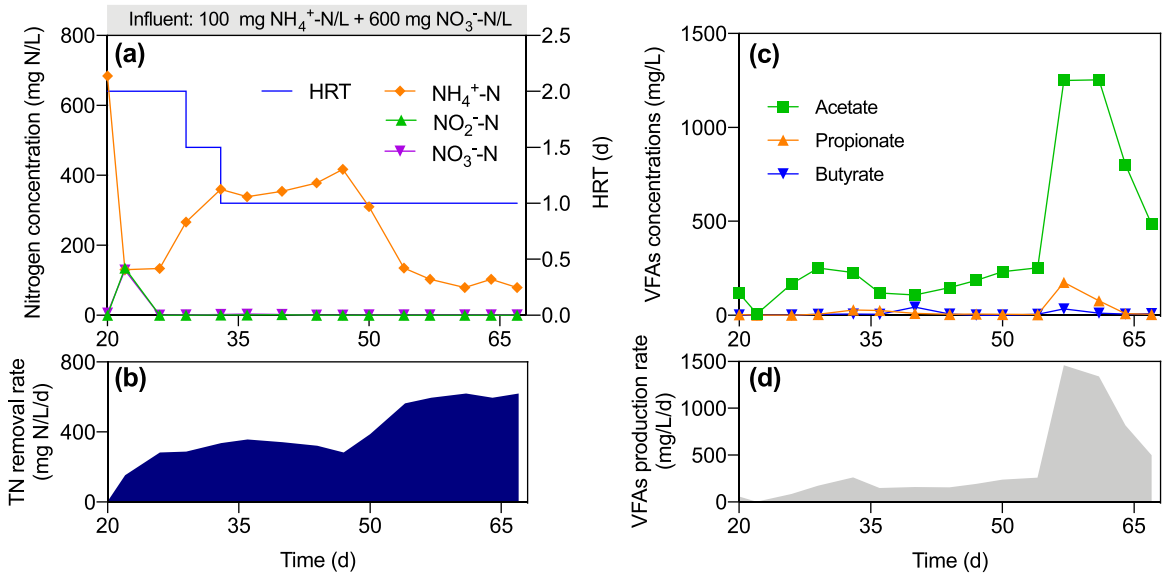

Fig. 2. Nitrogen removal and VFA production in Stage I of the syngas-based MBfR: (a) nitrogen profiles in the influent and effluent; (b) total nitrogen (TN) removal rate; (c) VFA profiles in effluent; and (d) VFA production rate.

indicating effective suppression of methanogens. However, the present study utilised a mixture of activated and anaerobic digestion sludge, without adding any inhibitors, and operated at a maintained neutral pH. With the exclusion of potential influencing factors such as inhibitors and pH, the suppression of methanogens in this system was likely attributed to other reasons. First, nitrate provision may inhibit the methanogenic pathway, as observed in previous studies [1,5]. However, despite its high concentration in the feed (~600 mg N/L) in Stage I, the *in situ* nitrate concentration in the bioreactor was always < 1 mg N/L. Moreover, methane production remained limited after nitrate was removed from the feed in Stage II (see Section 3.2). Thus, nitrate provision was unlikely to be the primary cause of the suppressed methanogenic activity. Another potential reason is substrate diffusion in counter-diffusion biofilms [37,38,58]. In the syngas-based MBfR, H_2 and CO_2 penetrated the biofilm substratum to the surface, whereas nitrate diffused in the opposite direction. Thus, denitrification-generating alkalinity occurs in the outer layer of the biofilms, whereas syngas fermentation-generating protons occur in the inner layer. Therefore, the pH of the biofilm should be lower than that of the bulk liquid, resulting in the suppression of methanogens. A similar pH gradient was reported in the counter-diffusion biofilms of an MBfR fuelled with oxygen [59], which showed that the in-biofilm pH was 4–6 while that in the bulk liquid was > 7. Unfortunately, with the current reactor design intended for a proof-of-concept study, obtaining intact biofilm samples to measure the pH gradient in biofilms was challenging. Although this study showed the feasibility of converting syngas to VFAs without using specific strategies to suppress methanogenic pathways, the actual mechanisms require further investigation.

3.2. Chromate reduction in syngas-based MBfR

Following the enrichment of nitrate-reducing biofilm, the continuous feeding of chromate with a concentration in the range of 18.7–21.5 μM was initiated on day 68. Nitrate and ammonium were no longer supplied

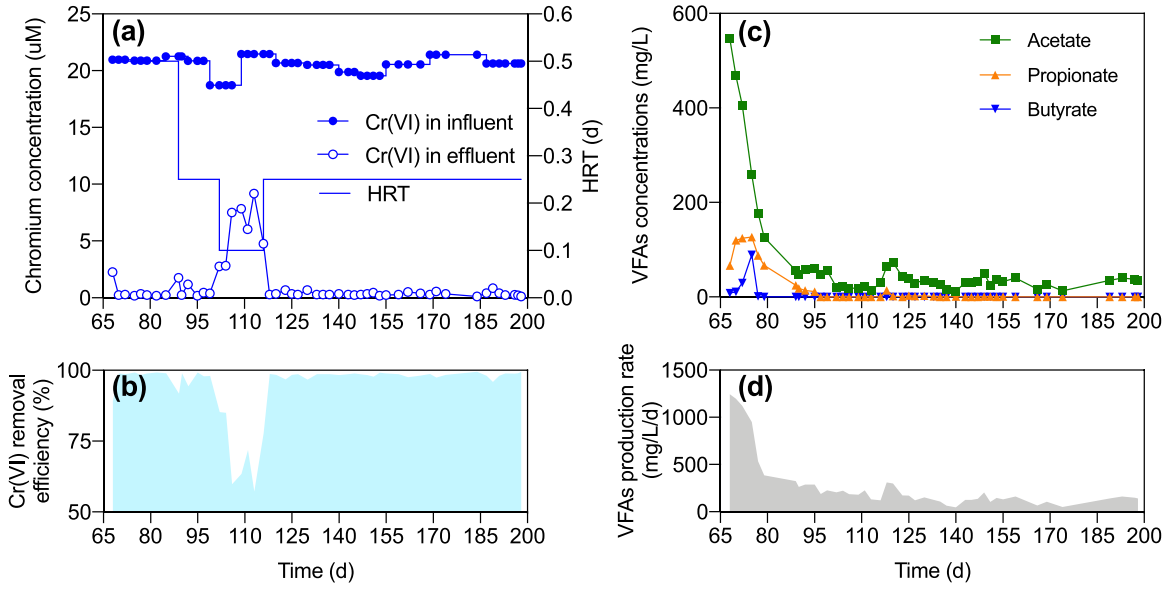

Fig. 3. Chromate removal and VFA production in Stage II of the syngas-based MBfR: (a) chromate profiles in the influent and effluent; (b) chromate removal efficiency; (c) VFA profiles in the effluent; and (d) VFA production rate.

during Stage II. Remarkably, without any acclimation at an HRT of 0.5 days, immediate and nearly complete chromate removal was observed (Fig. 3a). Therefore, the HRT was halved to 0.25 days after day 89. Despite the minor fluctuations, the average chromate removal efficiency remained > 95% (Fig. 3b). On day 102, the HRT was reduced to 0.1 days, resulting in an increase in effluent Cr(VI) concentration to 7–9 μmol/L and a decrease in chromate removal efficiency to 50–80%. Despite the reduced efficiency, the chromate removal rate increased from 80 μmol/L/d at a HRT of 0.25 days to 120 μmol/L/d at a HRT of 0.1 days. To improve the effluent quality, the HRT was increased back to 0.25 days on day 116, leading to a significant decrease in effluent chromate concentration, thereby achieving nearly complete chromate removal again. The syngas-based MBfR was operated under steady-state conditions for approximately 3 months, maintaining stable and high-level chromate removal. Throughout the operational period, soluble Cr(III) in the effluent could be detected, but at a markedly lower concentration (< 5.0 μmol/L) than that of the Cr(VI) in the influent (20.0 μmol/L) (Fig. S1). This suggests that most of the reduced Cr existed in the form of precipitates. Notably, the soluble Cr(III) in the effluent was inconsistent for different MBfRs. Although the absence of soluble Cr(III) in the effluent has been observed in most methane-driven MBfRs [29], hydrogen-driven MBfRs generally yield an effluent containing soluble Cr(III) [14].

Concurrently, the VFA production was monitored during Stage II. Considering the lower concentration of chromate compared to the nitrate supply in Stage II, the partial pressure of the syngas was further reduced to 1.1 atm at the beginning of Stage II. As a result of this adjustment and the shortened HRT, the VFA concentration in the effluent rapidly declined from > 500 mg/L to < 100 mg/L within 10 days (Fig. 3c–d). From day 89, the acetate concentration fluctuated at approximately 20–50 mg/L, whereas propionate and butyrate were scarcely detected. During the period with an HRT of 0.1 days (days 102–113), the effluent acetate concentration decreased to a lower level of 10–20 mg/L. Of note, the low effluent acetate concentration was mainly due to the short HRT applied in this period, while the corresponding acetate production rate was comparable to the previous stage at HRT of 0.25 days. Moreover, the percentage of methane in the off-gas was consistently < 3% at this stage, suggesting that the methanogenic pathway was still effectively suppressed. Particularly, the residual VFAs in the effluent were subject to the production from gas fermentation and the consumption in chromate removal. Thus, while showing the production of VFAs and the removal of chromate, the long-term results were unable to reveal whether these two processes were coupled. To address this question, *in situ* and *ex situ* batch tests were further conducted as elaborated in Section 3.4.

3.3. Tracing the speciation of Cr

SEM and EDS were applied after the long-term operation to reconfirm the production of Cr(III) from Cr(VI). Fig. 4 illustrates the morphology (Fig. 4a&c) and EDS spectrum (Fig. 4b&d) of Cr precipitates in biofilms collected from the membrane of the syngas-based MBfR. Cr (VI) is soluble in the influent, and no deposition of Cr should be observed in the inoculated sludge. On day 198, after operating the syngas-based MBfR for Cr(VI) removal for around 130 days, the EDS spectrum found clear Cr signals (*e.g.*, peaks located at around 587.5 eV), indicating the reduction of Cr(VI) to Cr(III) within the MBfR, which resulted in its precipitation and subsequent deposition on the biofilms attached to the hollow fibre membrane. This analysis confirmed that Cr(III) compounds were the major products of the reduction of Cr(VI) in the syngas-based MBfR.

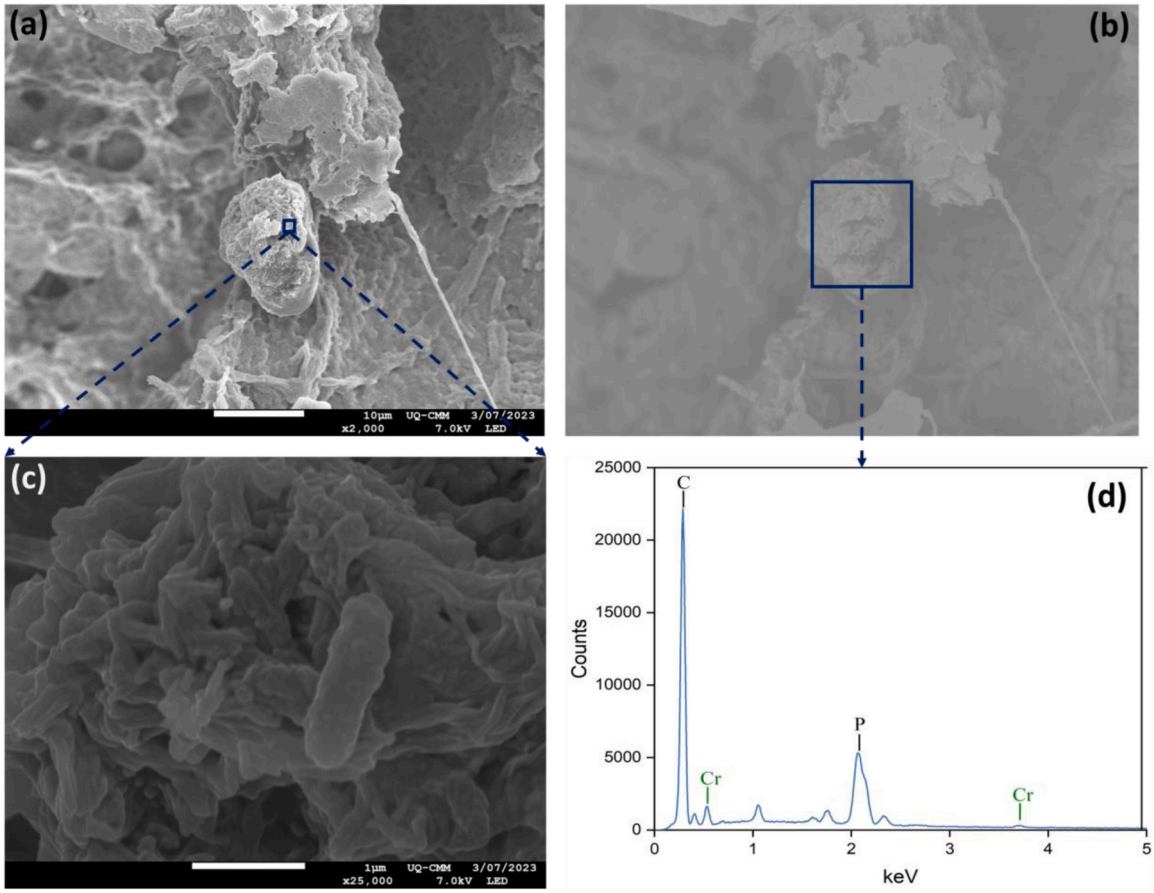

Fig. 4. SEM image (a&c) and EDS results (b&d) of the Cr precipitate in the biofilm.

3.4. *In situ and ex situ batch tests shed light on the mechanisms*

Five sets of *in situ* and *ex situ* batch tests were performed to elucidate the mechanisms underlying chromate removal in the syngas-based MBfR (Fig. 5). Batch test A served as the positive control in the presence of both syngas and VFAs. The reactor was periodically dosed with chromate for five consecutive cycles (Fig. 5a). The initial Cr(VI) concentration of each cycle ranged from 5 to 30 μmol/L, all of which exhibited consistent reduction within a timeframe of 4 to 8 h and followed a comparable trajectory. Previous studies on MBfRs fuelled by methane or short-chain alkanes have shown persistence in reducing oxidised pollutants such as nitrate and selenate, even in the absence of these gaseous electron donors [11,28]. This phenomenon was attributed to the potential utilisation of intracellular storage compounds, such as poly--β-hydroxybutyrate, to drive the reduction of oxidised pollutants [11,28]. To determine whether the microorganisms enriched in the syngas-driven MBfR have a similar capability to leverage intracellular compounds for chromate reduction, batch test B was performed without syngas and VFAs. Under such conditions, the biofilm-driven chromate reduction rate amounted to 6 μmol/L/d (Fig. 5b). This value was an order of magnitude lower than the reduction rate observed in batch test A, and constituted 3.7% of the rate observed in the long-term experiment. In another control group batch C where acetate was present but syngas was absent, the correlation between acetate and Cr(VI) consumption was evident, with a Cr(VI) reduction rate similar to that observed in Batch test A (Fig. S2). Collectively, these results substantiate the pivotal roles of syngas and VFAs in chromate removal.

In addition to the VFAs produced from syngas fermentation, the H_2 present in syngas can also function as a direct electron donor, driving chromate reduction [14,48]. To investigate the principal contributor orchestrating chromate bioreduction within the syngas-based MBfR, biofilms were harvested and subjected to *ex situ* batch tests. The first group was provided with H_2 only (batch test D), whereas the second group was provided with both H_2 and CO_2 (batch test E). As expected, H_2 was consumed in batch tests D and E at different rates (Fig. 5c and d). In particular, the simultaneous consumption of H_2 and CO_2 was observed in batch test E at a molar consumption ratio of 2.4:1, which is slightly higher than the theoretical syngas conversion ratio to acetate (2:1).

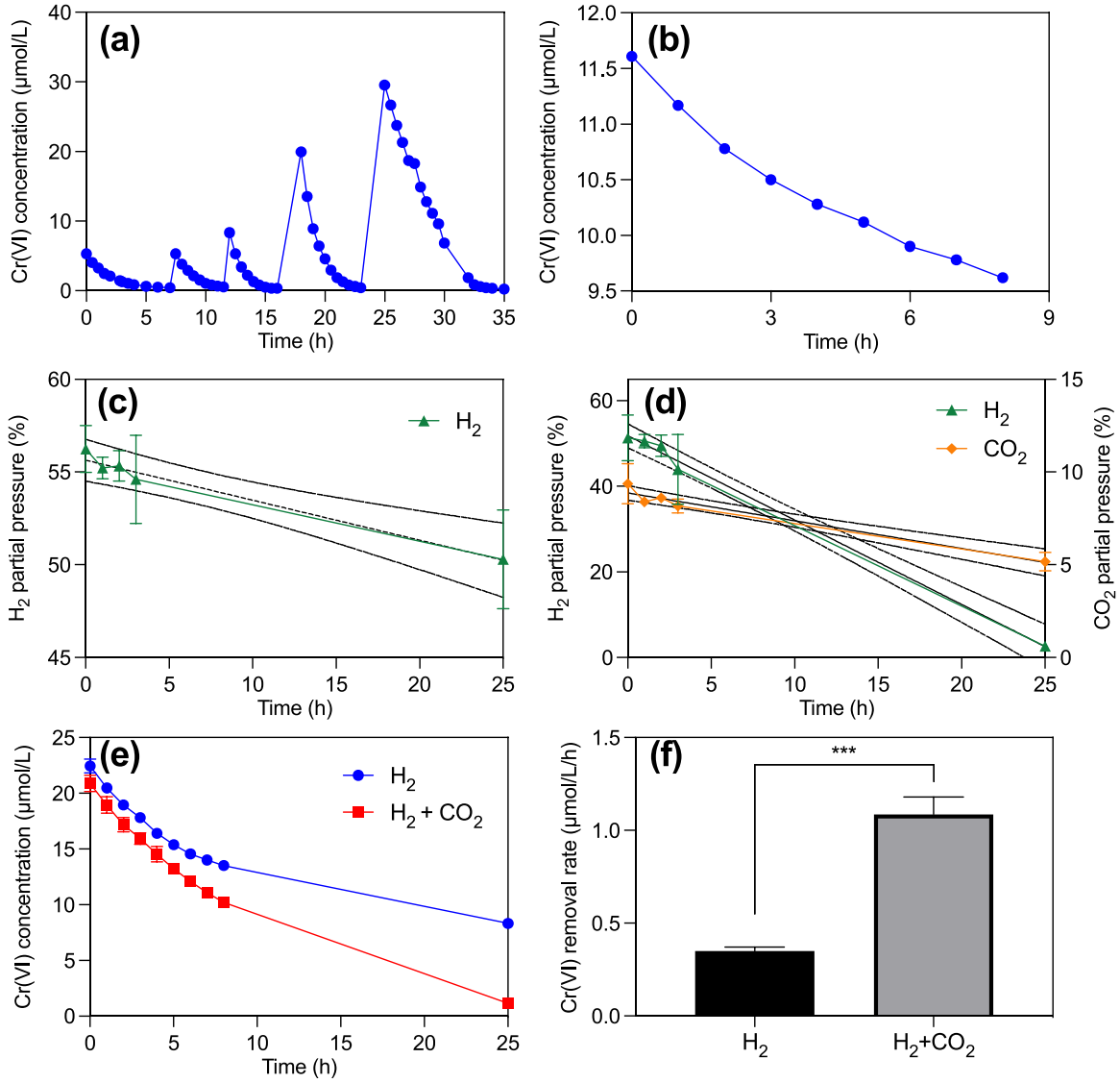

Fig. 5. *In situ* and *ex situ* batch tests results. (a) Chromate reduction in the *in situ* batch test A in the presence of syngas and VFAs; (b) chromate reduction in the *in situ* batch test B in the absence of syngas and VFAs; (c) profiles of H_2 in the *ex situ* batch test C with 50 mL H_2 added; (d) profiles of H_2 and CO_2 in the *ex situ* batch test D with 50 mL H_2 and 10 mL CO_2 added; (e) profiles of chromate in the *ex situ* batch tests C and D; and (f) chromate reduction rate in the *ex situ* batch tests C and D. The measured H_2 and CO_2 profiles were fitted using the linear equation with the dash lines corresponding to parameter values at a 95% confidence interval. Data points represent the mean values of biological triplicates and error bars indicate the standard deviation of the triplicates.

Furthermore, the chromate concentration decreased in both *ex situ* batch tests (Fig. 5e). However, the chromate reduction rate in batch test E was more than twice that in batch test D ($p < 0.001$) (Fig. 5f). Collectively, these findings led to the conclusion that the chromate reduction observed in the syngas-based MBfR was primarily steered by VFAs stemming from syngas fermentation. However, the contribution of direct H_2 utilization in syngas represented a relatively minor role in this process.

3.5. Variations in microbial communities

The microbial populations responsible for nitrate reduction, chromate reduction, and syngas fermentation were investigated using 16 S rRNA gene amplicon sequencing at the end of Stages I and II. At the phylum level, the biofilm community was mainly dominated by Proteobacteria, Firmicutes, and Bacteroidota, totally accounting for > 60% of the community (Fig. 6a). At the class level, the biofilm community consisted of various taxa, including Gammaproteobacteria, Methanobacteria, Negativicutes, Bacteroidia, Methanosarcinia, Anaerolineae, and Clostridia, totally accounting for > 90% of the community (Fig. 6b). Gammaproteobacteria contains broad denitrifying populations, which was also observed in many previous studies focusing on chromate reduction [26,62,79]. Bacteroidia has been detected as dominant in previous fermentation systems [54,83], which is proposed to be capable of performing gas fermentation. In addition, both Clostridia and Negativicutes members are known to be capable of reverse beta-oxidation, which may also trigger chain elongation in the system [8].

At the genus level, these populations were categorised based on their potential functions (Fig. 6c). First, a diverse range of heterotrophs that can utilise organics, such as *Pseudomonas* [9], *Thauera* [12,73,81], *Acidovorax* [33], *Rhodanobacter* [21], *Comamonas* [35], and *Proteiniphilum* [32,78], were detected in both stages. In terms of chromate reduction, Deinococci (a class) and *Meiothermus* (a genus within the class Deinococci), previously assumed to be associated with chromate reduction in methane-based MBfRs [29,43,82], were rarely present (< 0.1%) in the current system. Instead, there was a significant increase in the relative abundance of *Aquitalea* from 1.5% in Stage I to 60.5% in Stage II. *Aquitalea* is a genus that encompasses diverse species with the capability to utilise organic carbon, such as acetate [31]. Although enrichment of *Aquitalea* after replacing nitrate with chromate has been observed, its specific potential for chromate reduction remains unexplored. *Sporomusa* emerged as the dominant syngas fermenter, with a relative abundance ranging from 1.7% to 2.3% [2,46]. Additionally, *Clostridium*, another common genus capable of converting syngas to VFAs, exhibited a modest increase in relative abundance, from < 0.1% to 0.3%. Finally, the relative abundance of methanogen *Methanobrevibacter* decreased from 26.8% to 1.4%, further supporting the observation of a suppressed methanotrophic pathway.

However, it should be noted that the correlation between microbial relative abundance and activity can be weak [32,38]. Therefore, directly linking the activity of functional microorganisms (gas fermenters and chromate reducers) to their relative abundances based on amplicon sequencing results is difficult. Amplicon sequencing can only offer a broad perspective of microbial community structure and cannot pinpoint the specific functional microorganisms involved in gas fermentation and chromate reduction. It is also incapable of accurately identifying which functional enzymes mediate gas fermentation and chromate reduction. To gain a deeper understanding of the functional microbial community and the interactions among different groups (gas fermenters and chromate reducers), more sophisticated molecular approaches like metagenomics and metatranscriptomics should be utilised in future research.

3.6. Proposed pathways of syngas-driven chromate bio-reduction

This study introduced a novel avenue for chromate reduction by harnessing electron donors derived from syngas. While previous studies predominantly focused on single electron donor (Table 1), hybrid electron donors involving VFAs generated from gas fermentation and H_2

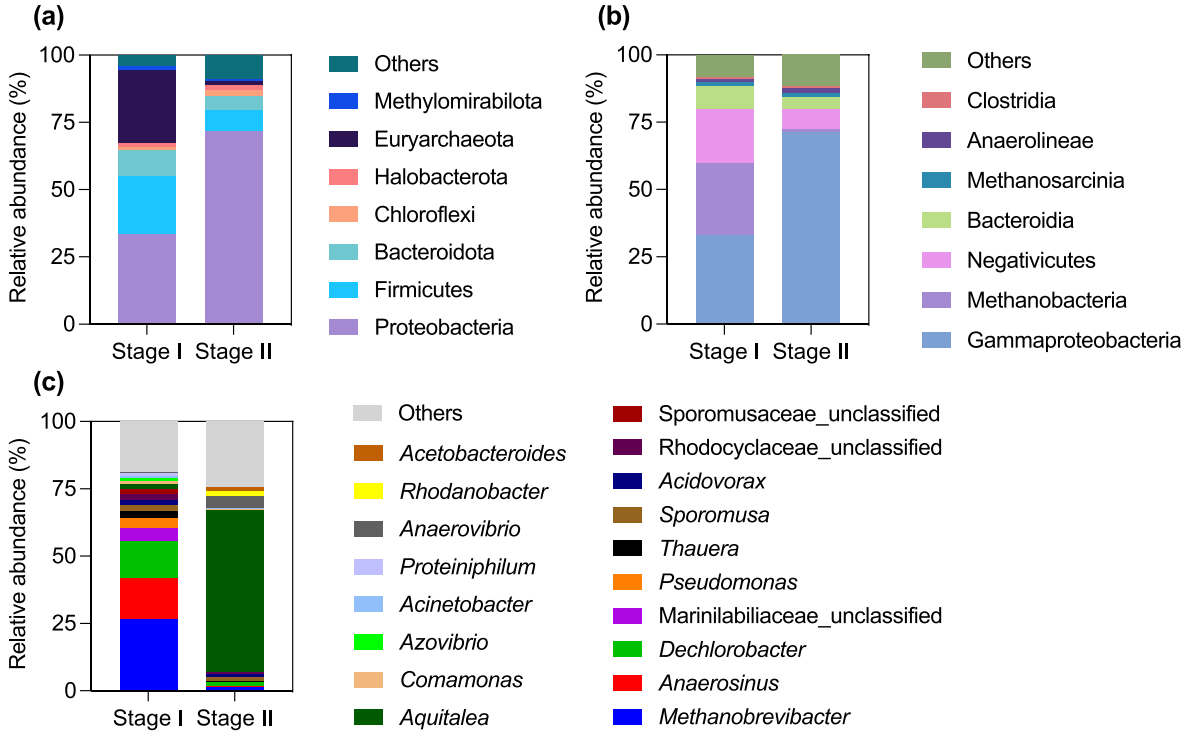

Fig. 6. Relative abundances of microbial communities at the end of Stage I and Stage II at the phylum (a), class (b), and genus level (c). Only the phylum, class, and genus that account for ≥ 1% of at least one sample are shown.

Table 1
Comparison between hydrogen-, methane-, ethane-, and syngas-based MBfRs for chromate removal.

Type of MBfR	Influent Cr (VI) (μmol/L)	Effluent Cr (VI) (μmol/L)	Removal rate of Cr (VI) (μmol/L/d)	Removal efficiency of Cr (VI)	References
CH_4-based MBfR	~20	< 1.0	~6	> 90%	[42]
	~58	< 0.5	~690	> 95%	[29]
	~77	< 0.5	~918	> 99%	[82]
	~38	< 0.5	~19	> 98%	[39]
H_2-based MBfR	~20	~8.0	~720	~60%	[14]
	~5	< 0.5	~900	> 95%	[15]
C_2H_6-based MBfR	~15	< 1.0	~6	> 95%	[13]
Syngas-based MBfR	20	< 0.5	120	> 95%	This study

originally present in the syngas were used for chromate reduction. Due to different electron sources, the pathway of chromate reduction in the present system was distinct from previous studies. Drawing on long-term performance, batch experiments, and analysis of the microbial community structure, this study articulates a mechanistic framework delineating syngas-driven chromate reduction (Fig. 7). This intricate pathway orchestrates synergistic interactions between fermentative microbial cohorts and a consortium of chromate-reducing microorganisms. The *in situ* fermentation of syngas results in VFA synthesis. Subsequently, these VFAs have emerged as critical electron donors during microbial chromate reduction. This concept is analogous to the pathways proposed for CH_4-driven nitrate reduction, where CH_4 is first fermented to VFAs [11,41]. However, the conversion of syngas into VFAs is more straightforward *via* the well-known Wood–Ljungdahl pathway than the currently unconfirmed pathway for CH_4 fermentation.

The postulated pathway appears to be intricately affected by the microbial stratification of MBfR biofilms. Syngas penetrates the biofilm from its base, whereas oxidised contaminants (such as nitrate and chromate) diffuse from the biofilm surface. This partitioning entails the likelihood of syngas fermentation occurring primarily within the inner layer of the biofilm, whereas the biological reduction of chromate occurs predominantly in its outer layers. In the inner biofilm, in which chromate is absent, fermenting bacteria exhibit a distinct preference for H_2 and CO_2 as substrates, yielding VFAs as metabolic products. Along with the gradual consumption of H_2 and CO_2, the synthesised VFAs permeate towards the outer layers, thus participating in the microbially driven reduction of chromate. For an exhaustive understanding of the precise pathway, future studies will require microscale analysis of the biofilm matrix.

3.7. Efficient chromate removal in syngas-based MBfR

Although previous studies have demonstrated the feasibility of using methane [29,39,42,82], short-chain alkanes [13], and hydrogen gas [14,15] as alternatives to traditional organic carbon (*e.g.*, ethanol) to remove chromate in water systems (Table 1), the feasibility of employing syngas as a substrate for microbial-driven chromate removal is reported here for the first time. A maximum chromate removal rate of approximately 120 μmol/L/d was obtained, which is comparable to that achieved in MBfRs fuelled by other gaseous substrates (Table 1). It should be noted that obtaining a high chromate removal rate was not the aim of the present study; thus, the gas supply was controlled at a very low level. Considering the high VFA production rate achieved in the initial stage of this study, it is tempting to speculate that with optimisation (*e.g.*, increasing the gas supply), the present technology has the potential to achieve a high chromate removal rate. Notably, chromate is a common contaminant in groundwater [70], which constitutes a primary drinking water source for ~33% and ~70% of the population in the United States and China [25,52], respectively. Compared to conventional organic carbon sources, such as ethanol, syngas, which is a renewable product generated from waste gasification, is a more economical resource for contaminant removal [76].

Indeed, syngas utilisation holds substantial promise for addressing pressing environmental challenges [10,64]. However, some notable constraints persist. First, syngas can be directly harnessed as a fuel source in gas engines, albeit with limitations due to its relatively low volumetric energy density [19]. Alternatively, the transformation of syngas into value-added chemicals has been explored as an attractive avenue [4,23]. However, the intrinsic value of primary products, such as acetate and ethanol, remains constrained, and their extraction from broth necessitates energy-intensive methodologies. Recently, extensive attention has been paid to upgrading short-chain fatty acids into more valuable, extractable, medium-chain products (*e.g.*, butyrate and caproate) [22,27]. However, to the best of our knowledge, significant fundamental and engineering knowledge gaps limit their practical applications. In this study, a novel avenue for syngas utilisation was

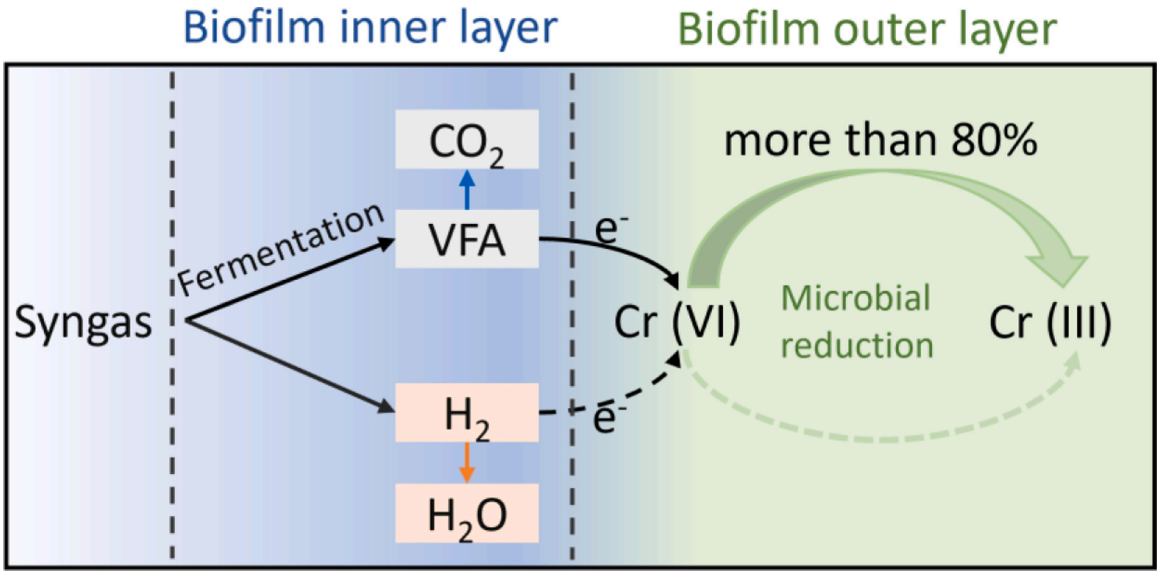

Fig. 7. Proposed pathways of syngas-based chromate removal.

introduced. This novel approach leverages the primary products of syngas fermentation, that is, acetate, for *in situ* contaminant remediation. This advantage is particularly evident when considering the challenges associated with separating and extracting various VFAs originating from syngas.

4. Conclusions

In summary, this study introduced an innovative approach for the effective removal of chromate from water using a syngas-based MBfR integrated with *in situ* fermentation. The primary findings of this study are as follows.

- Demonstrated long-term chromate removal: the syngas-based MBfR exhibited promising chromate removal capabilities with a high removal rate of approximately 120 μmol/L/d and a high removal efficiency exceeding 95%.
- Mechanisms underpinning chromate removal in the syngas-based MBfR: *in situ* syngas fermentation by gas fermenters (*e.g.*, *Sporomusa* and *Clostridium*) led to the generation of VFAs, which served as the primary drivers for microbial chromate removal by organics-utilising bacteria (*e.g.*, *Aquitalea*). The direct use of H_2 in the syngas for chromate reduction was relatively minor.

This study proposes an economically viable approach for effectively eliminating chromate from water systems using syngas as feedstock. This method establishes a new avenue for harnessing syngas, a renewable resource derived from biomass or sludge, and presents opportunities for sustainable resource utilisation.

CRediT authorship contribution statement

Chunyu Lai: Writing – original draft. **Yifeng Ying:** Investigation, Writing – review & editing. **Xinyu Zhao:** Investigation. **Mengxiong Wu:** Writing – original draft. **Danting Shi:** Writing – review & editing. **Tao LIU:** Writing – review & editing, Writing – original draft, Supervision, Conceptualization. **Chenkai Niu:** Writing – original draft, Investigation. **Jianhua Guo:** Writing – review & editing. **Shihu Hu:** Writing – review & editing.

Declaration of Competing Interest

The authors declare that they have no known competing financial interests or personal relationships that could have appeared to influence the work reported in this paper.

Data Availability

Data will be made available on request.

Acknowledgments

Dr. Tao Liu is the recipient of an Australian Research Council (ARC) DECRA Fellowship (DE220101310). Mr. Chenkai Niu acknowledges the support from the China Scholarship Council (CSC).

Appendix A. Supporting information

Supplementary data associated with this article can be found in the online version at doi:10.1016/j.jhazmat.2024.134195.

References

[1] Akunna, J.C., Bernet, N., Moletta, R., 1998. Effect of nitrate on methanogenesis at low redox potential. Environ Technol 19 (12), 1249–1254.
[2] Ammam, F., Tremblay, P.-L., Lizak, D.M., Zhang, T., 2016. Effect of tungstate on acetate and ethanol production by the electrosynthetic bacterium Sporomusa ovata. Biotechnol biofuels 9, 1–10.
[3] Asatiani, N.V., Abuladze, M.K., Kartvelishvili, T.M., Bakradze, N.G., Sapojnikova, N.A., Tsibakhashvili, N.Y., et al., 2004. Effect of chromium (VI) action on Arthrobacter oxydans. Curr Microbiol 49, 321–326.
[4] Bae, J., Jin, S., Kang, S., Cho, B.-K., Oh, M.-K., 2022. Recent progress in the engineering of C1-utilizing microbes. Curr Opin Biotechnol 78, 102836.
[5] Banihani, Q., Sierra-Alvarez, R., Field, J.A., 2009. Nitrate and nitrite inhibition of methanogenesis during denitrification in granular biofilms and digested domestic sludges. Biodegradation 20, 801–812.
[6] Barnhart, J., 1997. Occurrences, uses, and properties of chromium. Regul Toxicol Pharmacol 26 (1), S3–S7.
[7] Branco, R., Cristovao, A., Morais, P.V., 2013. Highly sensitive, highly specific whole-cell bioreporters for the detection of chromate in environmental samples. PLoS One 8 (1), e54005.
[8] Candry, P., Ganigué, R., 2021. Chain elongators, friends, and foes. Curr Opin Biotechnol 67, 99–110.
[9] Carlson, C.A., Ingraham, J.L., 1983. Comparison of denitrification by Pseudomonas stutzeri, Pseudomonas aeruginosa, and Paracoccus denitrificans. Appl Environ Microbiol 45 (4), 1247–1253.
[10] Centi, G., Quadrelli, E.A., Perathoner, S., 2013. Catalysis for CO 2 conversion: a key technology for rapid introduction of renewable energy in the value chain of chemical industries. Energy Environ Sci 6 (6), 1711–1731.
[11] Chen, H., Liu, S., Liu, T., Yuan, Z., Guo, J., 2020. Efficient nitrate removal from synthetic groundwater via in situ utilization of short-chain fatty acids from methane bioconversion. Chem Eng J, 124594.
[12] Chen, H., Liu, T., Li, J., Mao, L., Ye, J., Han, X., et al., 2020. Larger Anammox Granules not only Harbor Higher Species Diversity but also Support More Functional Diversity. Environ Sci Technol 54 (22), 14664–14673.
[13] Chi, Z., Ju, S., Wang, W., Li, H., Luo, Y.-H., Rittmann, B.E., 2023. Ethane-driven chromate and nitrate bioreductions in a membrane biofilm reactor. Chem Eng J 452, 139135.
[14] Chung, J., Nerenberg, R., Rittmann, B.E., 2006. Bio-reduction of soluble chromate using a hydrogen-based membrane biofilm reactor. Water Res 40 (8), 1634–1642.
[15] Chung, J., Rittmann, B.E., Wright, W.F., Bowman, R.H., 2007. Simultaneous bio-reduction of nitrate, perchlorate, selenate, chromate, arsenate, and dibromochloropropane using a hydrogen-based membrane biofilm reactor. Biodegradation 18, 199–209.
[16] Devarapalli, M., Atiyeh, H.K., Phillips, J.R., Lewis, R.S., Huhnke, R.L., 2016. Ethanol production during semi-continuous syngas fermentation in a trickle bed reactor using Clostridium ragsdalei. Bioresour Technol 209, 56–65.
[17] Diender, M., Stams, A.J., Sousa, D.Z., 2016. Production of medium-chain fatty acids and higher alcohols by a synthetic co-culture grown on carbon monoxide or syngas. Biotechnol biofuels 9, 1–11.
[18] Fernández, P.M., Viñarta, S.C., Bernal, A.R., Cruz, E.L., Figueroa, L.I., 2018. Bioremediation strategies for chromium removal: current research, scale-up approach and future perspectives. Chemosphere 208, 139–148.
[19] Fiore, M., Magi, V., Viggiano, A., 2020. Internal combustion engines powered by syngas: a review. Appl Energy 276, 115415.
[20] Ganguli, A., Tripathi, A., 2002. Bioremediation of toxic chromium from electroplating effluent by chromate-reducing Pseudomonas aeruginosa A2Chr in two bioreactors. Appl Microbiol Biotechnol 58, 416–420.
[21] Green, S.J., Prakash, O., Jasrotia, P., Overholt, W.A., Cardenas, E., Hubbard, D., et al., 2012. Denitrifying bacteria from the genus Rhodanobacter dominate bacterial communities in the highly contaminated subsurface of a nuclear legacy waste site. Appl Environ Microbiol 78 (4), 1039–1047.
[22] Grootscholten, T., Dal Borgo, F.K., Hamelers, H., Buisman, C., 2013. Promoting chain elongation in mixed culture acidification reactors by addition of ethanol. Biomass Bioenergy 48, 10–16.
[23] Heffernan, J.K., Lai, C.-Y., Gonzalez-Garcia, R.A., Nielsen, L.K., Guo, J., Marcellin, E., 2023. Biogas upgrading using Clostridium autoethanogenum for value-added products. Chem Eng J 452, 138950.
[24] Jones, S.W., Fast, A.G., Carlson, E.D., Wiedel, C.A., Au, J., Antoniewicz, M.R., et al., 2016. CO_2 fixation by anaerobic non-photosynthetic mixotrophy for improved carbon conversion. Nat Commun 7 (1), 12800.
[25] Kenny, J.F., Barber, N.L., Hutson, S.S., Linsey, K.S., Lovelace, J.K., Maupin, M.A., 2009. Estimated use of water in the United States in 2005. US Geological Survey,.
[26] Kiran Kumar Reddy, G., Nancharaiah, Y., 2018. Sustainable bioreduction of toxic levels of chromate in a denitrifying granular sludge reactor. Environ Sci Pollut Res 25 (2), 1969–1979.
[27] Kucek, L.A., Spirito, C.M., Angenent, L.T., 2016. High n-caprylate productivities and specificities from dilute ethanol and acetate: chain elongation with microbiomes to upgrade products from syngas fermentation. Energy Environ Sci 9 (11), 3482–3494.
[28] Lai, C.-Y., Wu, M., Wang, Y., Zhang, J., Li, J., Liu, T., et al., 2021. Cross-feeding interactions in short chain gaseous alkane-driven perchlorate and selenate reduction. Water Res 200, 117215.
[29] Lai, C.-Y., Zhong, L., Zhang, Y., Chen, J.-X., Wen, L.-L., Shi, L.-D., et al., 2016. Bioreduction of chromate in a methane-based membrane biofilm reactor. Environ Sci Technol 50 (11), 5832–5839.
[30] Lara, P., Morett, E., Juárez, K., 2017. Acetate biostimulation as an effective treatment for cleaning up alkaline soil highly contaminated with Cr (VI). Environ Sci Pollut Res 24, 25513–25521.

[31] Lee, C.-M., Weon, H.-Y., Kim, Y.-J., Son, J.-A., Yoon, S.-H., Koo, B.-S., et al., 2009. Aquitalea denitrificans sp. nov., isolated from a Korean wetland. Int J Syst Evolut Microbiol 59 (5), 1045–1048.

[32] Li, J., Liu, T., McIlroy, S.J., Tyson, G.W., Guo, J., 2023. Phylogenetic and metabolic diversity of microbial communities performing anaerobic ammonium and methane oxidations under different nitrogen loadings. ISME Commun 3 (1), 39.

[33] Li, X., Wang, H., Zhang, Y., Hu, C., Yang, M., 2014. Characterization of the bacterial communities and iron corrosion scales in drinking groundwater distribution systems with chlorine/chloramine. Int Biodeterior Biodegrad 96, 71–79.

[34] Liew, F., Martin, M.E., Tappel, R.C., Heijstra, B.D., Mihalcea, C., Köpke, M., 2016. Gas fermentation—a flexible platform for commercial scale production of low-carbon-fuels and chemicals from waste and renewable feedstocks. Front Microbiol 7, 694.

[35] Lim, Z.K., Liu, T., Zheng, M., Yuan, Z., Guo, J., Hu, S., 2021. Versatility of nitrite/nitrate-dependent anaerobic methane oxidation (n-DAMO): first demonstration with real wastewater. Water Res, 116912.

[36] Liu, C., Luo, G., Wang, W., He, Y., Zhang, R., Liu, G., 2018. The effects of pH and temperature on the acetate production and microbial community compositions by syngas fermentation. Fuel 224, 537–544.

[37] Liu, T., Guo, J., Hu, S., Yuan, Z., 2020. Model-based investigation of membrane biofilm reactors coupling anammox with nitrite/nitrate-dependent anaerobic methane oxidation. Environ Int 137, 105501.

[38] Liu, T., Hu, S., Yuan, Z. and Guo, J. (2023) Microbial Stratification Affects Conversions of Nitrogen and Methane in Biofilms Coupling Anammox and n-DAMO Processes. Environmental Science & Technology.

[39] Long, M., Zhou, C., Xia, S., Guadiea, A., 2017. Concomitant Cr (VI) reduction and Cr (III) precipitation with nitrate in a methane/oxygen-based membrane biofilm reactor. Chem Eng J 315, 58–66.

[40] Lovley, D.R., Coates, J.D., 1997. Bioremediation of metal contamination. Curr Opin Biotechnol 8 (3), 285–289.

[41] Luo, J.-H., Chen, H., Yuan, Z., Guo, J., 2018. Methane-supported nitrate removal from groundwater in a membrane biofilm reactor. Water Res 132, 71–78.

[42] Luo, J.-H., Wu, M., Liu, J., Qian, G., Yuan, Z., Guo, J., 2019. Microbial chromate reduction coupled with anaerobic oxidation of methane in a membrane biofilm reactor. Environ Int 130, 104926.

[43] Lv, P.-L., Zhong, L., Dong, Q.-Y., Yang, S.-L., Shen, W.-W., Zhu, Q.-S., et al., 2018. The effect of electron competition on chromate reduction using methane as electron donor. Environ Sci Pollut Res 25, 6609–6618.

[44] Mabbett, A.N., Macaskie, L.E., 2001. A novel isolate of Desulfovibrio sp. with enhanced ability to reduce Cr (VI). Biotechnol Lett 23, 683–687.

[45] McLean, J., Beveridge, T.J., 2001. Chromate reduction by a pseudomonad isolated from a site contaminated with chromated copper arsenate. Appl Environ Microbiol 67 (3), 1076–1084.

[46] Möller, B., Oßmer, R., Howard, B.H., Gottschalk, G., Hippe, H., 1984. Sporomusa, a new genus of Gram-negative anaerobic bacteria including Sporomusa sphaeroides spec. nov. and Sporomusa ovata spec. nov. Arch Microbiol 139, 388–396.

[47] Monga, A., Fulke, A.B., Dasgupta, D., 2022. Recent developments in essentiality of trivalent chromium and toxicity of hexavalent chromium: implications on human health and remediation strategies. J Hazard Mater Adv 7, 100113.

[48] Nerenberg, R., Rittmann, B., 2004. Hydrogen-based, hollow-fiber membrane biofilm reactor for reduction of perchlorate and other oxidized contaminants. Water Sci Technol 49 (11-12), 223–230.

[49] Nie, W.-B., Ding, J., Xie, G.-J., Yang, L., Peng, L., Tan, X., et al., 2020. Anaerobic oxidation of methane coupled with dissimilatory nitrate reduction to ammonium fuels anaerobic ammonium oxidation. Environ Sci Technol 55 (2), 1197–1208.

[50] O'Brien, T.J., Ceryak, S., Patierno, S.R., 2003. Complexities of chromium carcinogenesis: role of cellular response, repair and recovery mechanisms. Mutat Res/Fundam Mol Mech Mutagen 533 (1-2), 3–36.

[51] Pavesi, T., Moreira, J.C., 2020. Mechanisms and individuality in chromium toxicity in humans. J Appl Toxicol 40 (9), 1183–1197.

[52] Qiu, J., 2011. China to spend billions cleaning up groundwater, American Association for the Advancement of. Science.

[53] Ramió-Pujol, S., Ganigué, R., Bañeras, L., Colprim, J., 2015. Incubation at 25C prevents acid crash and enhances alcohol production in Clostridium carboxidivorans P7. Bioresour Technol 192, 296–303.

[54] Reddy, M.V., Hayashi, S., Choi, D., Cho, H., Chang, Y.-C., 2018. Short chain and medium chain fatty acids production using food waste under non-augmented and bio-augmented conditions. J Clean Prod 176, 645–653.

[55] Riegler, P., Chrusciel, T., Mayer, A., Doll, K., Weuster-Botz, D., 2019. Reversible retrofitting of a stirred-tank bioreactor for gas-lift operation to perform synthesis gas fermentation studies. Biochem Eng J 141, 89–101.

[56] Sahinkaya, E., Kilic, A., Calimlioglu, B., Toker, Y., 2013. Simultaneous bioreduction of nitrate and chromate using sulfur-based mixotrophic denitrification process. J Hazard Mater 262, 234–239.

[57] Sakai, S., Nakashimada, Y., Inokuma, K., Kita, M., Okada, H., Nishio, N., 2005. Acetate and ethanol production from H2 and CO2by Moorella sp. using a repeated batch culture. J Biosci Bioeng 99 (3), 252–258.

[58] Satoh, H., Ono, H., Rulin, B., Kamo, J., Okabe, S., Fukushi, K.-I., 2004. Macroscale and microscale analyses of nitrification and denitrification in biofilms attached on membrane aerated biofilm reactors. Water Res 38 (6), 1633–1641.

[59] Shanahan, J.W., Semmens, M.J., 2015. Alkalinity and pH effects on nitrification in a membrane aerated bioreactor: an experimental and model analysis. Water Res 74, 10–22.

[60] Shen, H., Wang, Y., 1993. Characterization of enzymatic reduction of hexavalent chromium by Escherichia coli ATCC 33456. Appl Environ Microbiol 59 (11), 3771–3777.

[61] Shi, J., Zhang, B., Qiu, R., Lai, C., Jiang, Y., He, C., et al., 2019. Microbial chromate reduction coupled to anaerobic oxidation of elemental sulfur or zerovalent iron. Environ Sci Technol 53 (6), 3198–3207.

[62] Shi, X., He, C., Lu, J., Guo, H., Zhang, B., 2022. Concurrent anaerobic chromate bio-reduction and pentachlorophenol bio-degradation in a synthetic aquifer. Water Res 216, 118326.

[63] Smith, W.A., Apel, W.A., Petersen, J.N., Peyton, B.M., 2002. Effect of carbon and energy source on bacterial chromate reduction. Bioremed J 6 (3), 205–215.

[64] Song, C., 2006. Global challenges and strategies for control, conversion and utilization of CO_2 for sustainable development involving energy, catalysis, adsorption and chemical processing. Catal Today 115 (1-4), 2–32.

[65] Speight, J.G., 2019. Unconventional gas. Nat Gas 59–98.

[66] Standeven, A.M., Wetterhahn, K.E., 1991. Is there a role for reactive oxygen species in the mechanism of chromium (VI) carcinogenesis? Chem Res Toxicol 4 (6), 616–625.

[67] Sutton, D., Kelleher, B., Ross, J.R., 2001. Review of literature on catalysts for biomass gasification. Fuel Process Technol 73 (3), 155–173.

[68] Tang, Y., Ziv-El, M., Meyer, K., Zhou, C., Shin, J.H., Ahn, C.H., et al., 2012. Comparing heterotrophic and hydrogen-based autotrophic denitrification reactors for effluent water quality and post-treatment. Water Sci Technol: Water Supply 12 (2), 227–233.

[69] Testa, S.M., Guertin, J., Jacobs, J., Avakian, C. (2004) Sources of chromium contamination in soil and groundwater, CRC Press: Boca Raton, FL, pp143–164.

[70] Tumolo, M., Ancona, V., De Paola, D., Losacco, D., Campanale, C., Massarelli, C., et al., 2020. Chromium pollution in European water, sources, health risk, and remediation strategies: an overview. Int J Environ Res Public Health 17 (15), 5438.

[71] Vatsouria, A., Vainshtein, M., Kuschk, P., Wiessner, A., Kaestner, M., 2005. Anaerobic co-reduction of chromate and nitrate by bacterial cultures of Staphylococcus epidermidis L-02. J Ind Microbiol Biotechnol 32 (9), 409–414.

[72] Vögeli, B., Schulz, L., Garg, S., Tarasava, K., Clomburg, J.M., Lee, S.H., et al., 2022. Cell-free prototyping enables implementation of optimized reverse β-oxidation pathways in heterotrophic and autotrophic bacteria. Nat Commun 13 (1), 3058.

[73] Wang, B., Qiao, X., Hou, F., Liu, T., Pang, H., Guo, Y., et al., 2022. Pilot-scale demonstration of a novel process integrating Partial Nitritation with simultaneous Anammox, Denitrification and Sludge Fermentation (PN+ ADSF) for nitrogen removal and sludge reduction. Sci Total Environ 815, 152835.

[74] Wang, S., Liu, C., Wang, X., Yuan, D., Zhu, G., 2020. Dissimilatory nitrate reduction to ammonium (DNRA) in traditional municipal wastewater treatment plants in China: Widespread but low contribution. Water Res 179, 115877.

[75] Wieringa, K., 1939. The formation of acetic acid from carbon dioxide and hydrogen by anaerobic spore-forming bacteria. Antonie Van Leeuwenhoek 6, 251–262.

[76] Wu, M., Lai, C.-Y., Wang, Y., Yuan, Z., Guo, J., 2023. Microbial nitrate reduction in propane-or butane-based membrane biofilm reactors under oxygen-limiting conditions. Water Res 235, 119887.

[77] Xu, S., Fu, B., Zhang, L., Liu, H., 2015. Bioconversion of H 2/CO 2 by acetogen enriched cultures for acetate and ethanol production: the impact of pH. World J Microbiol Biotechnol 31, 941–950.

[78] Yang, Q., Zhao, N., Wang, H., Huang, B., Yan, Q., 2020. Electrochemical and biochemical profiling of the enhanced hydrogenotrophic denitrification through cathode strengthening using bioelectrochemical system (BES). Chem Eng J 381, 122686.

[79] Zhang, B., Liu, J., Sheng, Y., Shi, J., Dong, H., 2021. Disentangling microbial syntrophic mechanisms for hexavalent chromium reduction in autotrophic biosystems. Environ Sci Technol 55 (9), 6340–6351.

[80] Zhang, F., Ding, J., Zhang, Y., Chen, M., Ding, Z.-W., van Loosdrecht, M.C., et al., 2013. Fatty acids production from hydrogen and carbon dioxide by mixed culture in the membrane biofilm reactor. Water Res 47 (16), 6122–6129.

[81] Zheng, M., Li, H., Duan, H., Liu, T., Wang, Z., Zhao, J., et al., 2023. One-year stable pilot-scale operation demonstrates high flexibility of mainstream anammox application. Water Res X, 100166.

[82] Zhong, L., Lai, C.-Y., Shi, L.-D., Wang, K.-D., Dai, Y.-J., Liu, Y.-W., et al., 2017. Nitrate effects on chromate reduction in a methane-based biofilm. Water Res 115, 130–137.

[83] Zhou, X., Lu, Y., Huang, L., Zhang, Q., Wang, X., Zhu, J., 2021. Effect of pH on volatile fatty acid production and the microbial community during anaerobic digestion of Chinese cabbage waste. Bioresour Technol 336, 125338.